

Article

Landscape Dynamics in the Caspian Lowlands Since the Last Deglaciation Reconstructed From the Pedosedimentary Sequence of Srednaya Akhtuba, Southern Russia

Marina Lebedeva ^{1,*} , Alexander Makeev ² , Alexey Rusakov ³, Tatiana Romanis ¹ ,
Tamara Yanina ⁴, Redzhep Kurbanov ^{4,5,6} , Pavel Kust ^{1,2}  and Evgeniy Varlamov ¹

¹ Laboratory of Soil Mineralogy and Micromorphology, V.V. Dokuchaev Soil Science Institute, Pyzhyovskiy Lane 7 Building 2, Moscow 119017, Russia; romanis.tatyana@yandex.ru (T.R.); pavelkust@yandex.ru (P.K.); evgheni968@rambler.ru (E.V.)

² Faculty of Soil Science, M.V. Lomonosov Moscow State University, Leninskie Gori, MSU, 1-12, Moscow 119992, Russia; makeevao@gmail.com

³ Institute of Earth Sciences, Saint Petersburg State University, 7-9, Universitetskaya nab, Saint Petersburg 199034, Russia; spp-06@mail.ru

⁴ Faculty of Geography, M.V. Lomonosov Moscow State University, Leninskie Gori, MSU, 1, Moscow 119992, Russia; didacna@mail.ru (T.Y.); roger.kurbanov@gmail.com (R.K.)

⁵ Laboratory of Evolutionary Geography, Institute of Geography RAS, Staromonetny, 29, Moscow 119017, Russia

⁶ Laboratory of Archaeomagnetism and the Earth's magnetic field evolution, Schmidt Institute of Physics of the Earth RAS, Bolshaya Gruzinskaya str., 10-1, Moscow 123242, Russia

* Correspondence: m_verba@mail.ru; Tel.: +7-962-979-40-45

Received: 6 November 2018; Accepted: 13 December 2018; Published: 16 December 2018



Abstract: Surface Kastanozem of the Lower Volga area was first studied as a part of the pedocomplex, with the lower part (148–160 cm) formed in Early Khvalynian Chocolate clays (13–15 ka), the middle part (100–148 cm) in a mixed clay-loess sediment sand, and the upper part (0–100 cm) in loess. This resulted from local aeolian transport, with the source material derived from the rewinding of marine sediments. They are enriched in aggregates of Chocolate clays and glauconitic grains of a fine sand-course silt size and have similar contents of clay minerals. The high salinity of similar types evidences marine genesis for both Chocolate clays and source material for loess sediments. Clay fragments of a sand and silt size are responsible for the heavy texture and high gypsum content of loess. The study of soils with the focus on micromorphology and clay mineralogy allows the identification of the complex character of a shift from marine to sub-areal sedimentation. This shift was accompanied by short breaks in sedimentation, allowing the development of synlithogenic soil horizons of Late Khvalynian, after-Khvalynian, and Boreal time. The features of shallowly buried soil horizons confirm increased aridity after the last deglaciation. Surface Calcic Kastanozem is a full Holocene soil reflecting the present environment. However, it is deeply influenced by shallow buried soil horizons and Chocolate clays.

Keywords: Caspian Lowland; Kastanozems; Chocolate clays; loess; pedocomplex; shallow buried soils

1. Introduction

The Caspian Lowland is a part of the extensive Ponto-Caspian basin that reflects fluctuations in the level of the Caspian and Black sea, glacial-interglacial cycling, and related fluctuations in fluvial activity

and aeolian sedimentation. The outcrops at the banks of the Volga River and its tributaries expose detailed Late Pleistocene pedosedimentary sequences, with marine, aeolian, and fluvial deposits intermixed with pedogenetic levels of interglacial and interstadial paleosols [1]. During the last deglaciation and degradation of permafrost, the Volga River basin collected meltwater and acted as a trap for fine-grained sediments from the southern margin of the Scandinavian ice-sheet [1–4]. That led to the Early Khvalynian transgressive stage(s) and induced the deposition of Chocolate clays—light-brown and dark-brown dense layers of heavy clays with a platy-prismatic structure that contain manganese and gypsum staining.

Chocolate clays are a unique sediment for the Caspian region. They were first described by Zhukov [5] as dark-brown deposits that, in the dry state, break up into tiles similar to chocolate bars. Currently, Chocolate clays are common for stratigraphic and paleogeographic schemes of the area. Chocolate clays a few meters thick on average could be located at the surface, forming the parent material for surface soils, or covered by marine (Caspian) sands or sandy loams [6,7]. In the Srednaya Akhtuba, Leninsk, and Raigorod sections (Figure 1), we found them covered by a thin (less than 1 m) layer of loess, so that surface soils (Calcic Kastanozems) are presented by a pedocomplex formed in loess underlain by Chocolate clays. An arid environment by the end of MIS 2 is reported in many publications. Subareal sedimentation during the Pleistocene/Holocene transition is a clear indication of an arid environment. However, it has not yet been studied enough. The goal of the present study is to examine intricate details of the shift from marine to subareal sedimentation recorded in the pedocomplex with surface Kastanozems in relation to the landscape evolution during the last deglaciation.



Figure 1. Study site area and spatial distribution of Chocolate clays in the Northern Caspian and Volga regions ([7], modified). The arrow points to the Srednaya Akhtuba study site.

2. Study Area

The study site (Srednaya Akhtuba section) is located at the left bank of Srednaya Akhtuba, a left distributary of the Volga river (48.7005277 N, 44.89330709 E) (Figure 1).

The study area is located in the dry steppe, with Calcic Kastanozems as a dominant soil. Kastanozem and Solonetz complexes, formed mostly in silty heavy loams, occupy the terrain between depressions. These complexes include: (1) Calcic Kastanozems under communities dominated by *Festuca valesiaca* or *Tanacetum achilleifolium*; (2) Haplic Kastanozems under polydominant meadow communities (*Stipa capillata*, *Medicago romanica*, *Veronica spicata*, Gramineae); and (3) Amphi-Salic Solonetz under *Artemisia pauciflora*–*Kochia prostrata* communities [8–12]. The soil pattern is strongly

dependent on the parent material and microtopography. In slightly visible depressions of a few cm, the dominant Kastanozems merge to Solonchaks or Solonetz. Within deeper depressions (limans), the soils cape pattern is composed of Eutric Planosols, Vertic Kastanozems, and Vertisols in Chocolate clays. The climate of the area is strongly continental, with a mean annual evaporation value (about 1000 mm) much higher than the mean annual precipitation (289 mm for the period 1952–1998). The mean annual temperature is +7.1 °C, with a maximum of +42 °C in summer and a minimum of −38 °C in winter [13]. The depth of soil freezing can reach 1 m.

The upper part of the sedimentary cover of the Lower Volga region is composed of diverse Quaternary sediments with varied thicknesses of several hundred meters [1]. A significant part of the section consists of various fluvial, marine, lacustrine, and lagoon deposits. Aeolian deposits locally represent continental sediments. The location of the region within a zone of permanent migration of the land-sea border and presence of the Volga river mouth predetermined a wide development of sediments of complicated genesis: alluvial-marine (deltaic), lake-sea (lacustrine and lagoonal), and lake-alluvial, consisting of various facies combined with each other laterally and vertically. Overlying sediments of the Atelian suite (MIS 4, Figure 2) are represented solely by continental or subaerial water formations—sandy-loam, less often sands, and loess deposits, interbedded with paleosols, also bearing traces of cryoturbation and lenses of lacustrine sediments enclosing shells of terrestrial and freshwater mollusks.

Early and Late Khvanynian are two transgressions, separated by Enotaevsk regression; they cover most of the surface of the Caspian lowland. They are divided into Lower and Upper Khvalynian sediments, as characterized by complexes of mollusks and separated by breaks in the continuity of sedimentation (Enotaevian regression). The lithofacies composition of the Lower Khvalynian deposits includes Chocolate clays and shallow sandy sediments, mostly related to depressions of a more ancient age. These sediments are abundant in various mollusks shells (*Dreissena polymorpha*, *Dr. rostriformis*, *Monodacna caspia*, *Hypanis plicata*, and characteristic Early Khvalynian species *Didacna ebersini*, *D. protracta*, *D. parallella*). Sandy interbeds are distributed throughout the clay unit, which suggests highly variable environments during sedimentation. According to the radiocarbon dates, the period of the Chocolate clay accumulation falls between 11 and 15 ka BP [14]. The Early Khvalynian plain that is now the second terrace of the Volga and Akhtuba Rivers is a closed-drainage terrain with a well-developed mesotopography that includes large depressions and wet estuaries (limans).

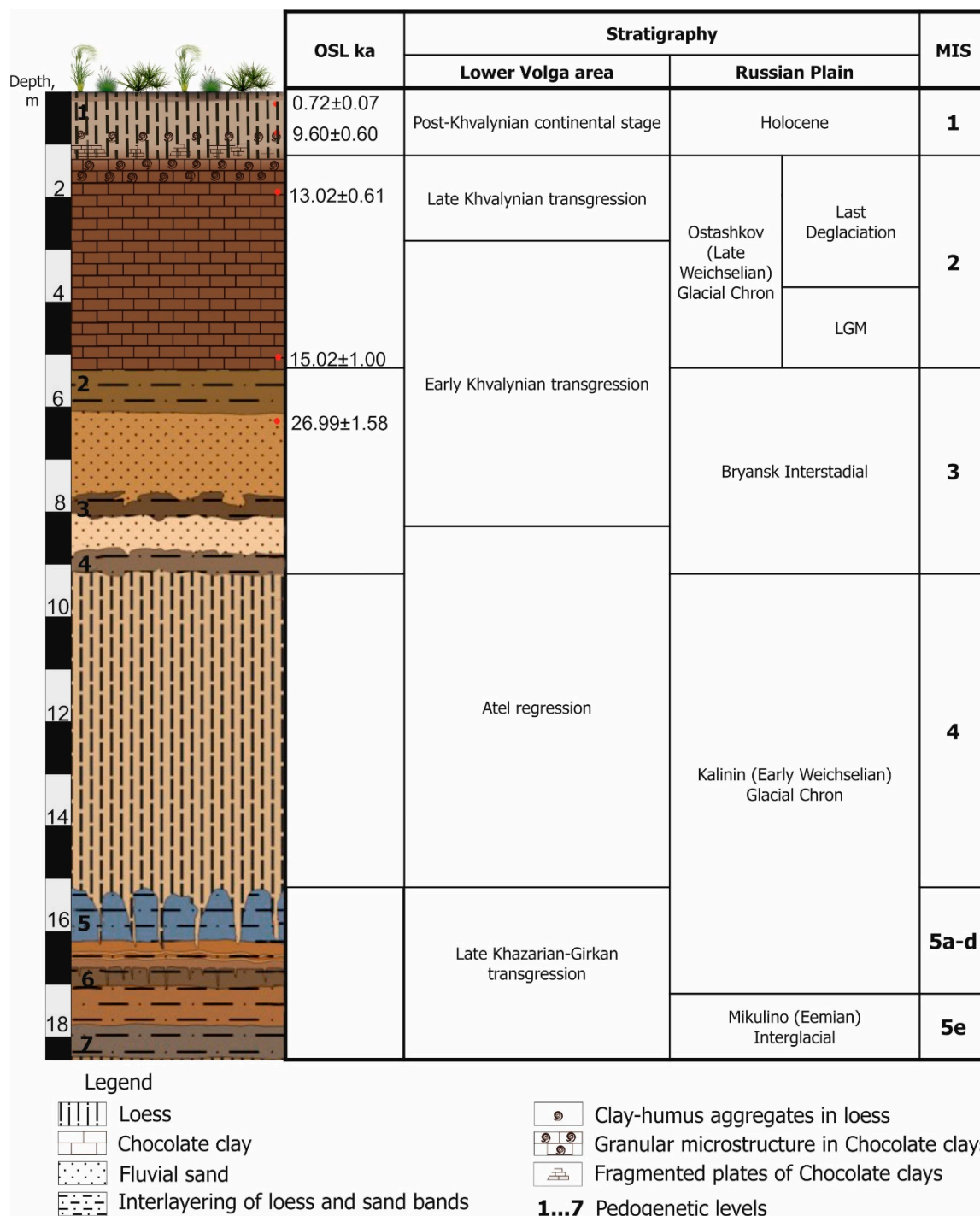


Figure 2. Chronostratigraphy of the pedosedimentary sequence in the Srednaya Akhtuba section. The upper part is shown in more detail in Figure 3. OSL dates are reported from [15,16].

The Srednaya Akhtuba section is a unique exposure representing the most complete sequence of Late Pleistocene continental and marine deposits interbedded with seven pedogenetic levels from MIS 5 to MIS 1 (Figure 2, [1,4,15,17–21]).

It is especially important that the Srednaya Akhtuba outcrop is confined within the area of Chocolate clays (Lower Khvalynian marine deposits) that are typical for the middle and lower reaches of the Volga River and its tributaries (Figure 1). Subaerial post-Khvalynian sediments constitute the upper part of the sequence. They are underlined by Chocolate clays. OSL dates of Chocolate clays determined for the studied section ($15,000 \pm 1000$ in the lower part and $13,000 \pm 500$ years in the upper

part, Figure 2) testify that they accumulated during the degradation of Ostashkov glacial Chron [15,22]. These data are in good agreement with the results of radiocarbon dating of mollusk shells, lying in the sand interlayers in the thickness of Chocolate clays of Lower Volga [23]. Surface soil formed in silty clay loam subareal sediments, underlain by Chocolate clays at a depth of 100 cm (Figure 3).

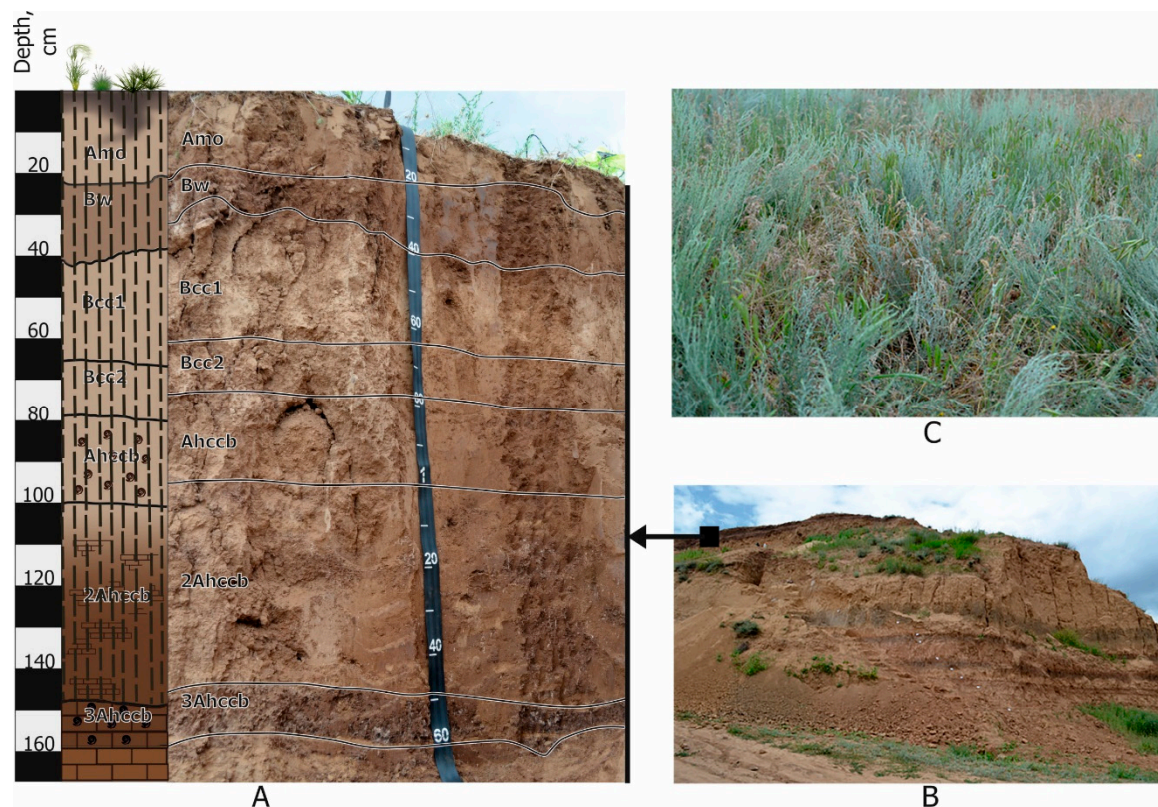


Figure 3. Srednaya Akhtuba study site. (A) Calcic Kastanozem; (B) General view of the Srednaya Akhtuba outcrop, with the pedosedimentary sequence presented in Figure 2; (C) Sagebrush vegetation typical for dry steppe.

3. Materials and Methods

Macro- and micromorphological studies. Surface soil was examined based on the study of exposure down to 2.5 m. Soil samples from all genetic horizons and underlying layers of Chocolate clays have been examined morphologically, according to the FAO Guidelines for Soil Description (2006) [24]. Soil color was determined in the field using Munsell Soil Color Charts (2013) [25]. Field identification of soil was determined using the IUSS Working Group WRB (2015) [26].

The thin sections were prepared by M.A. Lebedev at the Dokuchaev Soil Science Institute. The micromorphological analyses were conducted using standard techniques and an Olympus BX51 polarizing microscope with an Olympus DP26 digital camera. The soil micro fabrics were compared using large (4 × 5 cm) thin sections in two replications and also vertical cross-sections of samples collected from the main genetic horizons. Specialized computer software supplied with the Olympus BX51 microscope (Tokyo, Japan) was used for visualization of the features observed. International terminology was used for describing the soil fabric [27].

Laboratory studies. The grain size analysis for fine earth material (<1 mm) was conducted by the conventional pipette method [28] to appropriate texture classes. The particle size distribution was analyzed for Russian conventional fraction groups (Figure 10). Grain size analysis was also conducted by the laser diffraction method using the Frisch Analysette 22. Fractions <0.25 mm were studied and the distribution curves were produced. Textural classes were determined according to FAO Guidelines for soil description (2006) [24].

pH_{H2O} was determined using a potentiometer, in suspension with a soil to water ratio of 1:2.5, after a single shaking step followed by settling for 30 min. The composition of the water extract (1:5), Calcium carbonate content, gypsum, and exchangeable acidity were analyzed using conventional methods [29]. Calcium and Magnesium in the water extract were determined by complexometric titration, and Sodium and Potassium were detected by flame photometry. Total alkalinity was determined by titration with sulfuric acid on the indicator methyl orange. The content of chloride ions was determined by the argentometric method according to Moor, and the content of sulfate ions by precipitation titration according to Aidinyan. Exchange bases were determined by the Pfeffer method in the modification of Molodtsov and Ignatova [29]. The total content of sulfate ions was determined by the gravimetric method [30]. Salinity was assessed according to the criteria given in the monograph “Salt-affected soils of Russia” (2006) [31].

Organic carbon content was determined by the Tyurin method, which included the wet combustion of organic substance in a mixture of 0.4 N K₂Cr₂O₇ and concentrated H₂SO₄ (1:1) at 150 °C for 20 min. The measurements were performed by photometry on a SPECOL 211 spectrometer at 590 nm.

Clay minerals contents were determined for the clay fraction (<0.001 mm) that was extracted according to Gorbunov [32] and clay mineralogy was determined by X-ray diffractometer HZG-4B (Carl-Zeiss Jena) [33]. Carbonates and soluble salts were removed prior to fractionation. From the samples, oriented preparations were prepared on a glass substrate measuring 20 × 20 mm. Shooting mode: Cu radiation voltage on a tube 30 kV current strength 20 mA, the angular velocity of the counter 2° –2Θ per minute, final calculations were performed using software Diffractometer-Auto version 2014 developed by Iris LLC. Samples of minerals of fractions <1 μm were shot in duplicate with a displacement of the survey plane by 90° in order to reduce the effect of possible heterogeneity of the drug distribution. The ratio of the main mineral phases of the clay fraction was calculated using the Biscay method [34,35]. Mineral diagnostics was carried out according to the methodology described in [36–39].

4. Results

4.1. Field Morphology

Calcic Kastanozem formed under dry steppe communities dominated by *Festuca valesiaca* or *Tanacetum achilleifolium* (Figure 3). The soil profile is a pedocomplex with the upper part (0–100 cm) formed in loess, the middle part (100–148 cm) in clay-loess sediment, and the lower part (148–160 cm) in heavy clay. The soil profile is characterized by flaking steppe felt at the surface, followed by a light gray (7.5 YR6/2 in the upper part) to brown (7.5 YR 4/4 in the lower part) humus horizon of a 20 cm thickness. Uncovered coarse grains are visible in the upper part. The most colorful Cambic horizon with a strong brown “chestnut” color (7.5 YR 4/6) follows down to 40 cm, where it merges with Calcic horizons with a strong effervescence and high variability of secondary carbonates. It has a strong angular blocky and platy structure. Thin clay-humus coatings cover inter-horizon pores. A sequence of synlithogenic buried soil horizons starts at 100 cm. (Table 1).

The first synlithogenic soil horizon (80–100 cm) is formed in heavy loess, the second (100–148 cm) in a mixture of loess with abundant clay fragments, and the third (148–160 cm) in the upper layer of Chocolate clays. Chocolate clays are a poly-mineral formation consisting of: (1) monoclay layers of “Chocolate color”; (2) interlayers of soft thin yellow sands with mollusks shells (*Didacna Protracta*, *D. Ebersini*, *Dreissena Rostriformis*, *Dr. Polymorpha*); and (3) and (4) gray fine silty coatings on the surface of fine prismatic structural units (Figure 4).

Table 1. Field morphology of the studied soil *.

Horizon	Lower Boundary, cm	Colour of a General Matrix (moist)	Artifacts	Coatings	Salt Crystals	Structure	Carbonate Reaction	Forms of Secondary Carbonates	Forms of Secondary Gypsum	Type of Voids	Abundance of Roots	Horizon Boundary		Consistence
												Distinctness, cm	Topography	
Calcic Kastanozem														
L	0					Steppe litter						A		S
Amo1	9	7.5 YR6/2	N	–	–	GR(ME)WM + SB(ME)WM + PL(FI)WE	N	–	–	I-C, C-V	Common	G	S	VFR to LO
Amo2	20	7.5 YR 4/4	N	–	–	PL(ME)MS + SB(ME)WM	N	–	–	I-C, C-V	Many	C	W	VFR to FR
Bw	40	7.5 YR 4/6	ChC-F-V	CH, VT-F/THC	–	PS(FM)MO → AB(FI)WM	SL	–	–	I-C, C-V	Common	C	W	FI
Bcc1	65	7.5 YR 6/4	ChC-F-F	CH, VT-V/TCH	–	AB(ME)WM	ST	D, SC	–	I-F, C-V	Very few	C	W	FR to VFR
Bcc2	80	7.5 YR 4/6	ChC-C-F	CH, VT-V/TCH	Few	AB(ME)WM → PL(VM)WE	ST	D, SC	–	I-F, C-V	Many	C	W	FR
Ahccb	100	7.5 YR 5/4	ChC-M-M		Few	CR(MC)WE → AS(VM)WE	MO			I-F, C-M	Few	G	S	FI to FR
2Ahccb	148	7.5 YR 4/3	ChC-A-M	C, VT-V/P	Few	LU(MC)WE → AS(VM)WE	MO	–	D	I-F, C-V	Very few	A	S	FR
3Ahccb	160	7.5 YR 5/3	Sh-M-C	CH, VT-V/PV ST, T-M/P	Few	AP(MC)ST	MO		D	P-M	–	–	–	VFI

* Indexes are based on FAO guide for soil description [24]. **Coatings:** “nature, thickness-abundance/location (with modification: THC–on the walls on the transhorizon cracks)”; thickness: VT very thin (<0.2), T thin (0.2–0.5); **Structure:** “structure type (size class structure of pedal soil materials) & combinations of soil structures”. **Type of voids:** “Classification of voids-abundance”. **Modifications:** “–” no presented; **Artifacts:** “type- abundance-size” types: Sh–mollusc’s shells; ChC–fragments of Chocolate clays. **Consistence:** LO-Loose, VFR-Very friable, FR-Friable, FI-Firm, VFI-Very firm, EFI-Extremely firm.

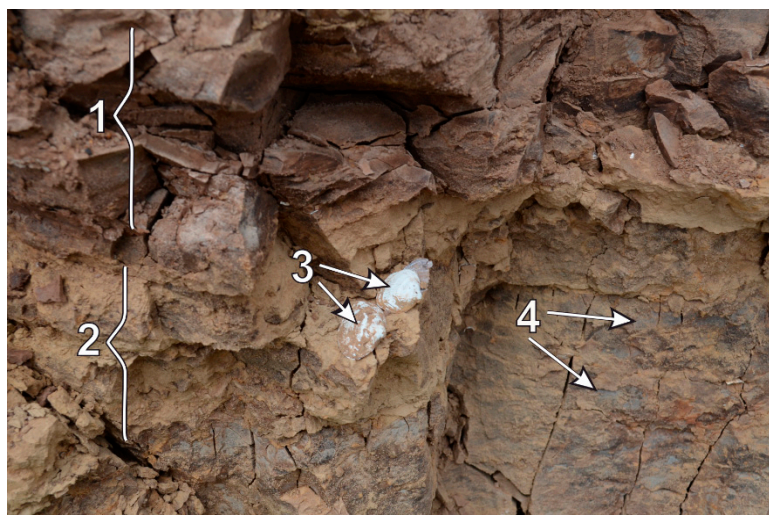


Figure 4. The facies of Chocolate clays: 1—mono clay layers of “Chocolate color”; 2—interlayers of thin yellow sands with mollusk shells; 3 and 4—gray fine silty coatings on the surface of fine prismatic structural units.

In the uppermost part, Chocolate clays are enriched with fine transparent gypsum crystals that are absent below. Manganese stains and Fe-Mn coatings are abundant in the lower part. In contrast to the upper boundary of Chocolate clays with loess, the lower boundary with underlying sediments is plain and sharp. (Figure 5).

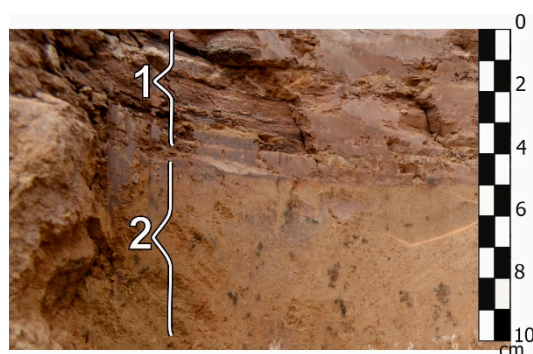


Figure 5. Sharp contact of Chocolate clays (1) with underlying loess and sand layers, MIS 3 (Figure 2).

4.2. Soil Micromorphology

A mono-clay layer (148–155 cm) with a strong brown color and granular microstructure inside angular prismatic aggregates (Figure 6A,B) presents the lower part of the pedocomplex; some of them look like coprolites (Figure 6C,D). There are microzones where micromass is characterized by high birefringence and monostriated b-fabric. Few gypsum crystals are present in the micromass.

The overlying layer (100–148 cm), clearly shows a mixture of clay with silt with quartz and feldspar grains. The platy fragments of Chocolate clays are enriched with fine silt (Figure 6E). This layer has the highest amount of gypsum crystals that are all confined to fragments of Chocolate clays. Big crystals have an irregular shape. Infillings with diamond-shaped gypsum crystals formed in adjacent pores. Biotubulars indicate the former activity of soil biota. Another sign of biota activity is the presence of biogenic pores—channels (Figure 6G,H).

The upper part of the pedocomplex (0–80 cm) is formed in silty clay loam that shows micro features typical of loess sediments: silty micromass with a granular microstructure and abundant pores (Figure 7A). Fragments of Chocolate clays of a fine sand and coarse silt size are abundant in the micromass (Figure 7B). Clay fragments are different in size, color, and grain size, like in different parts

of the main strata of Chocolate clays. The loess layer shows a different mineralogy—the presence of glauconitic grains, absent in the strata of Chocolate clays. Pedogenetic transformation of the lower loess layer and the presence of buried soil horizon of synlithogenic soil is evidenced by the aggregation of micromass with clay-humus aggregates, the presence of spores covered by clay coatings, abundant coal particles, colonies of iron bacteria, and earthworm casts (Figure 7C–F).

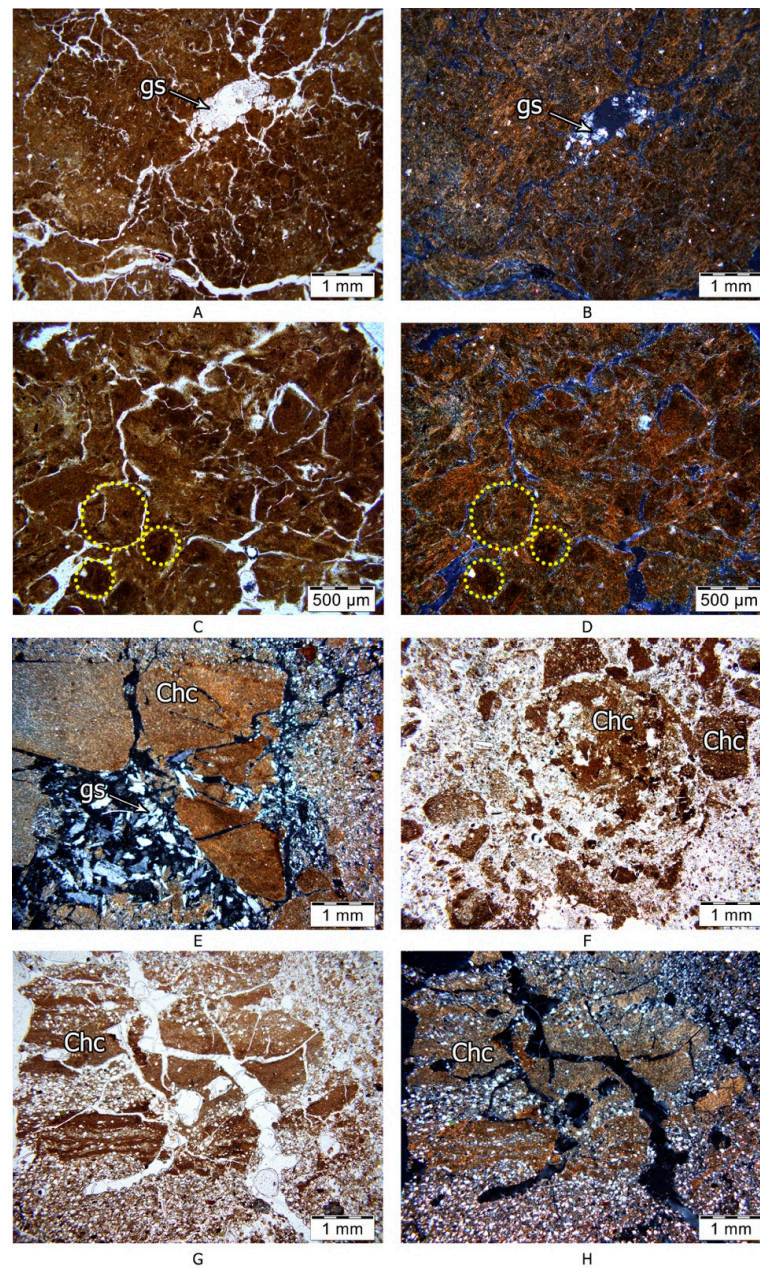


Figure 6. Sub-areal transformation of Chocolate clays. (A,B)—high birefringence and monostriated b-fabric of the micromass, granular microstructure, and gypsum crystals (gs) in pores (155 cm; (A)—PPL; (B)—XPL); (C,D)—rounded biogenic aggregates (155 cm; (C)—PPL, (D)—XPL); (E)—heterogeneous fragments of Chocolate clays (Chc), splitting of clay plates by gypsum (gs) crystals (100–148 cm, XPL); (F)—biotubula with fragments of Chocolate clays (Chc) (100–148 cm, PPL); (G,H)—fragmented plates of Chocolate clays, disintegrated by biogenic pores, in sorted silty micromass (100–148 cm, (G)—PPL; (H)—XPL).

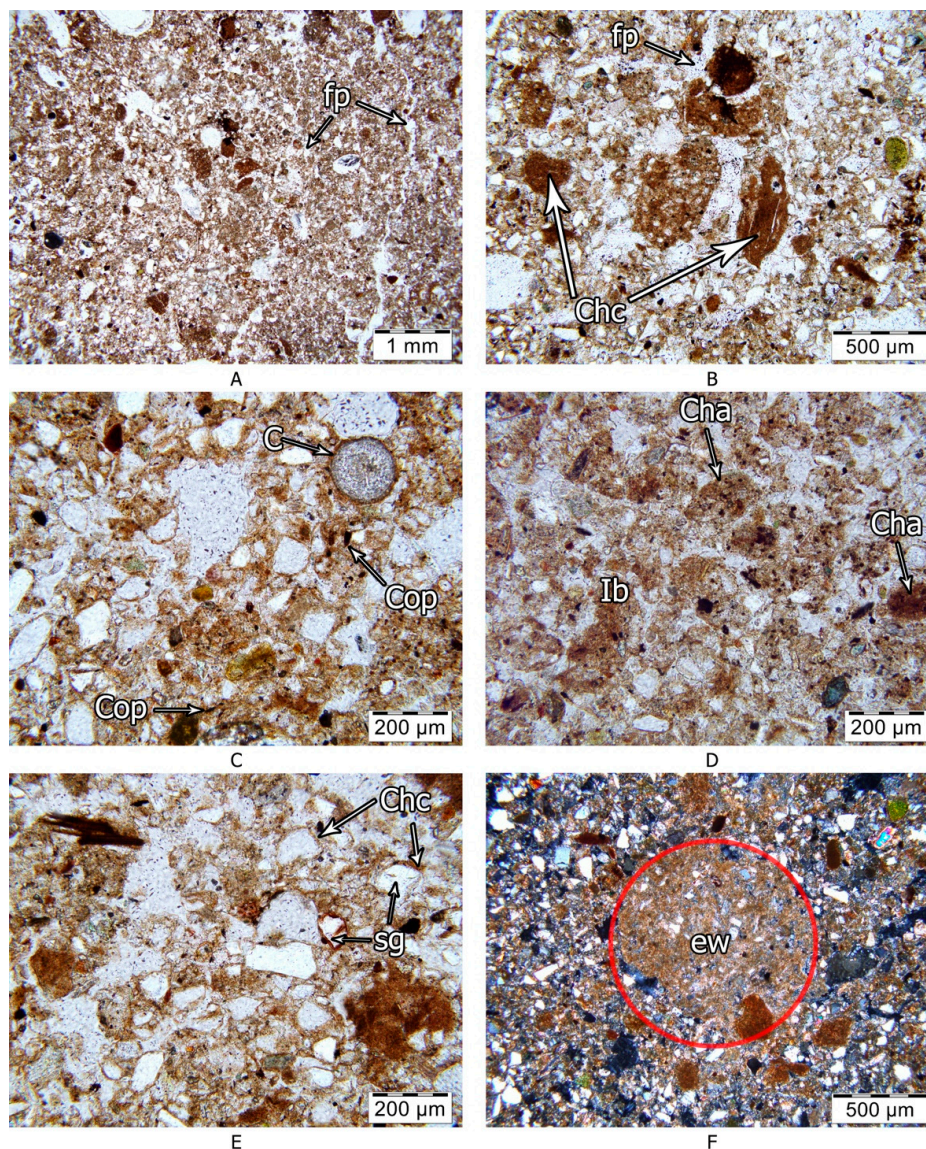


Figure 7. The microstructure of the lower part of the loess layer (80–100 cm): (A)—silty material with abundant fine pores (fp) and granular microstructure. Note abundant fragments of Chocolate clays of fine sand and coarse silt size. PPL; (B)—the same with higher magnification. Note clay fragments (Chc) of various shapes, colors, and grain sizes, and the presence of glauconitic grains, PPL; (C)—spore covered by clay coatings (C) and abundant coal particles (Cop), PPL; (D)—clay-humus aggregates (Cha) and colonies of iron bacteria (Ib), PPL; (E)—clay-humus coatings (Chc) on sand grains (sg), PPL; (F)—earth-worm (ew) cast filled with carbonate material of Chocolate clay, XPL.

Calcic horizons of Kastanozem at a depth of 80 to 40 cm below the day surface are formed in similar loess material (Figure 8A). They are characterized by the high content of carbonate neo-formations—micritic impregnation and soft nodules in the micromass (Figure 8C,D). The micromass is well-aggregated. The prismatic structure, shown in the field description, in the thin sections gives rectangular aggregates (Figure 8A). The abundance of clay fragments decreases compared to the lower horizons, and they are smaller and exclusively consist of dense mono-clay material (Figure 7B). Earthworm casts are visible in inter-horizon pores that are characteristic of Kastanozems (Figure 8A).

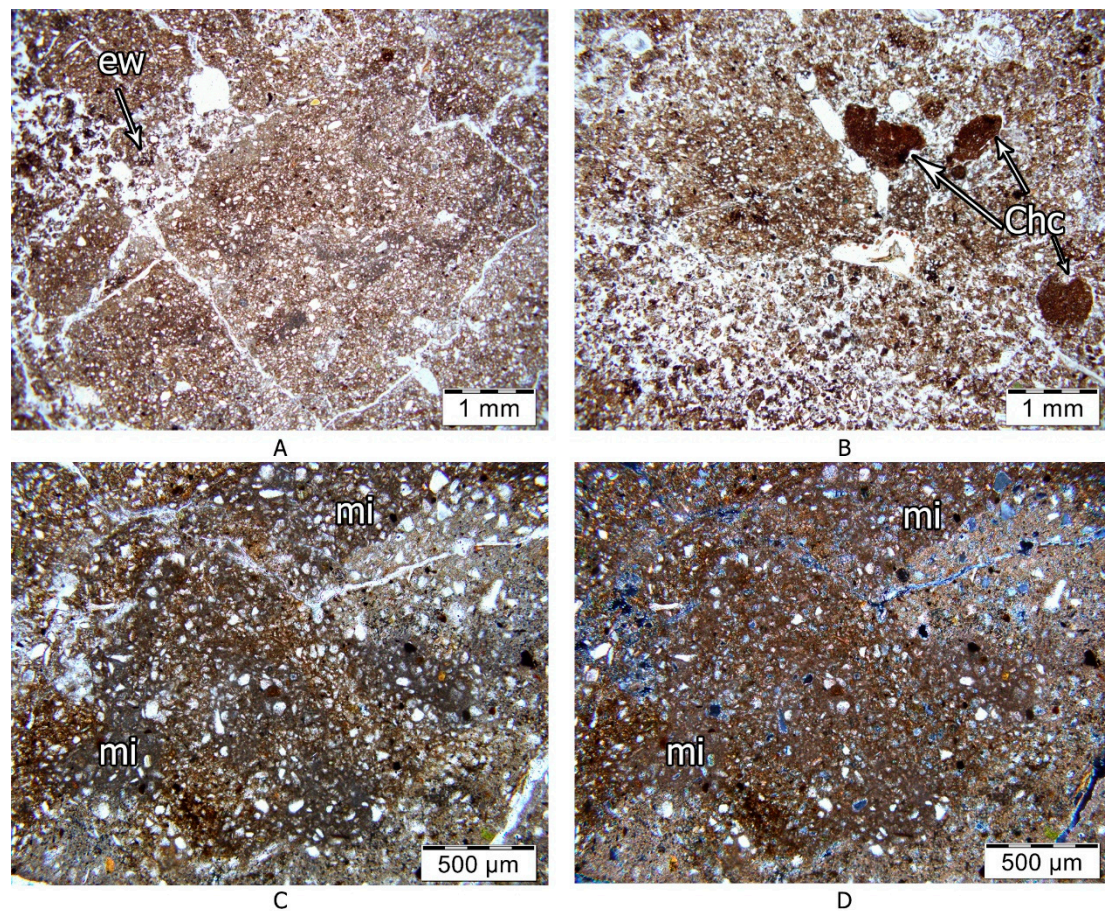


Figure 8. Microstructure of Calcic horizons. (A)—rectangular structure of silty-clay carbonate material with earth-worm (ew) casts (65–80 cm, PPL); (B)—silty-clay micromass with abundant fine fragments of Chocolate clays of various shapes (40–65 cm, PPL); (C,D)—heterogeneous micritic impregnation (mi) of the groundmass (65–80 cm, (C)—PPL, (D)—XPL).

Within the depth range of 20–40 cm (Bw horizon), modern carbonate pedofeatures such as coatings and micritic infillings are rarely found on the interior surface of fine and very fine voids (mostly channels) (Figure 9A,B). The Mollic horizon formed in the upper 20 cm has low aggregation and weak humus impregnation of the micromass that is typical of soils of arid environments. However, some rounded aggregates and earthworm casts are darker in color. Rounded aggregates tend to form plates; in some parts, a platy microstructure becomes dominant (Figure 9C,D). There are abundant grains of fine sand dispersed in the micromass. They also tend to form intermittent streaks of 1 mm thick (Figure 8C,D). Some of the sand grains are crashed (Figure 8F) and show a circular orientation (Figure 9D). Fine fragments of Chocolate clays are evenly dispersed in the micromass (Figure 9E,F). Plant tissue is impregnated with carbonates (Figure 9G,H).

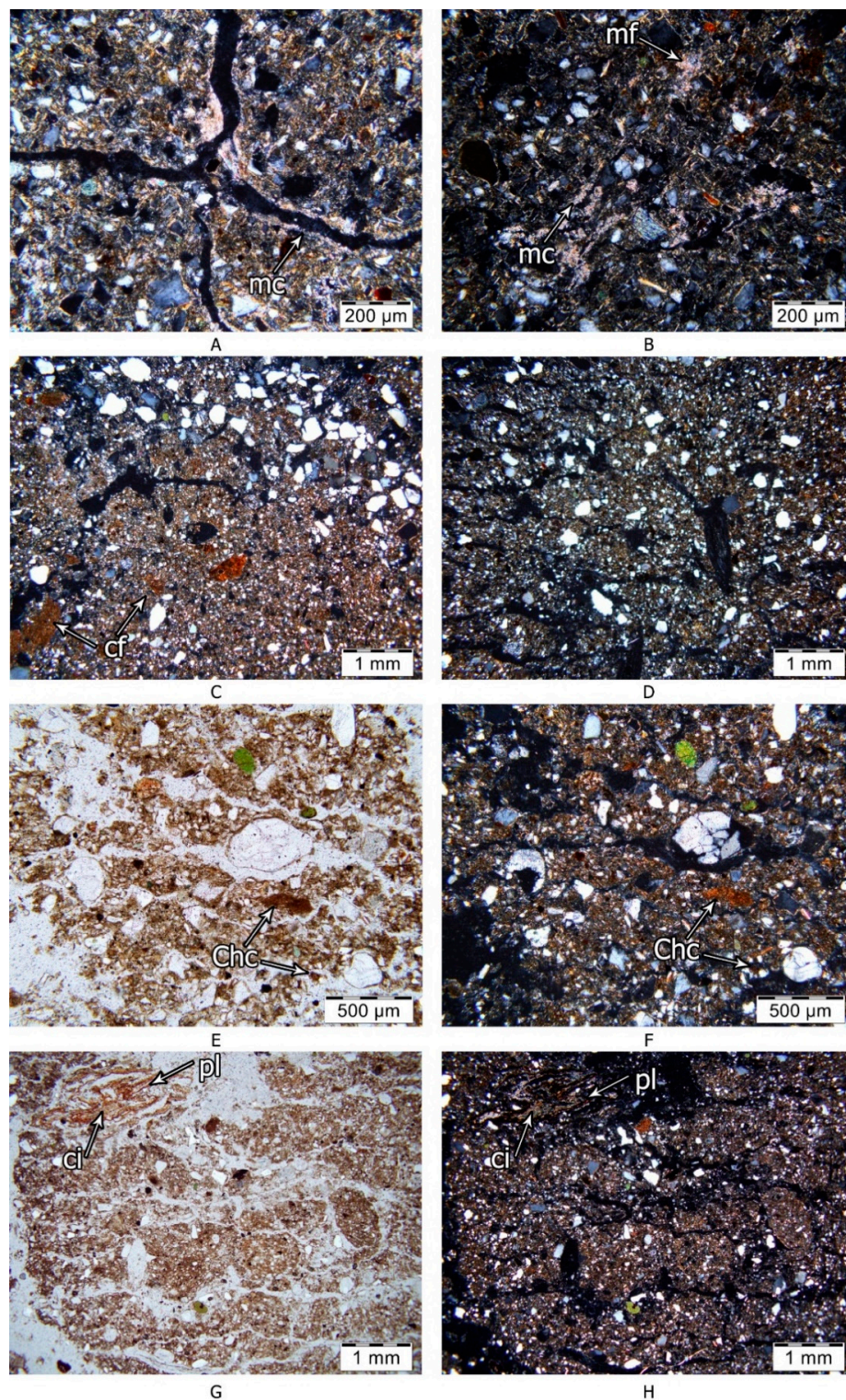


Figure 9. The microstructure of Mollic and Cambic horizons of Kastanozem: (A)—dense silty clay micromass with blocky aggregates, high birefringence, and thin micritic coatings (mc) (20–40 cm, XPL); (B)—thin micritic coatings (mc) and infillings (mf) in the micromass (20–40 cm, XPL); (C)—loose silty clay micromass with sand streaks and abundant clay fragments (cf) of various shapes (9–20 cm, XPL); (D)—transformation of rounded biogenic aggregates into thin platy aggregates and circular orientation (0–9 cm, XPL); (E,F)—loose silty-clay-humus micromass with sand grains and fine granular and platy microstructure. With rare fragments of Chocolate clays (Chc) (0–9 cm, e-PPL; f-XPL); (G), (H)—carbonate impregnation (ci) within plant (pl) tissue (0–9 cm, g-PPL; h-XPL).

4.3. Analytical Features

Grain size distribution (Figure 10) confirms that the pedocomplex includes several sediment layers. The lower part (148–160 cm) is formed in Silty clay that is typical for mono-clay layers of Chocolate clays. The upper part of the pedocomplex (0–100 cm) is formed in Silt loam and Silty clay loam with the high content of loess fraction (coarse silt) and fine sand that is typical for sandy loess sediments. Texture variability within the loess layer relates to the variable admixture of clay aggregates (see Section 4.2.). The admixture of sand grains in the upper 20 cm also correlates with microfeatures. In spite of abundant clay fragments recorded in the field and in thin sections, the texture of the middle part (100–148 cm) is similar to the overlying loess layer.

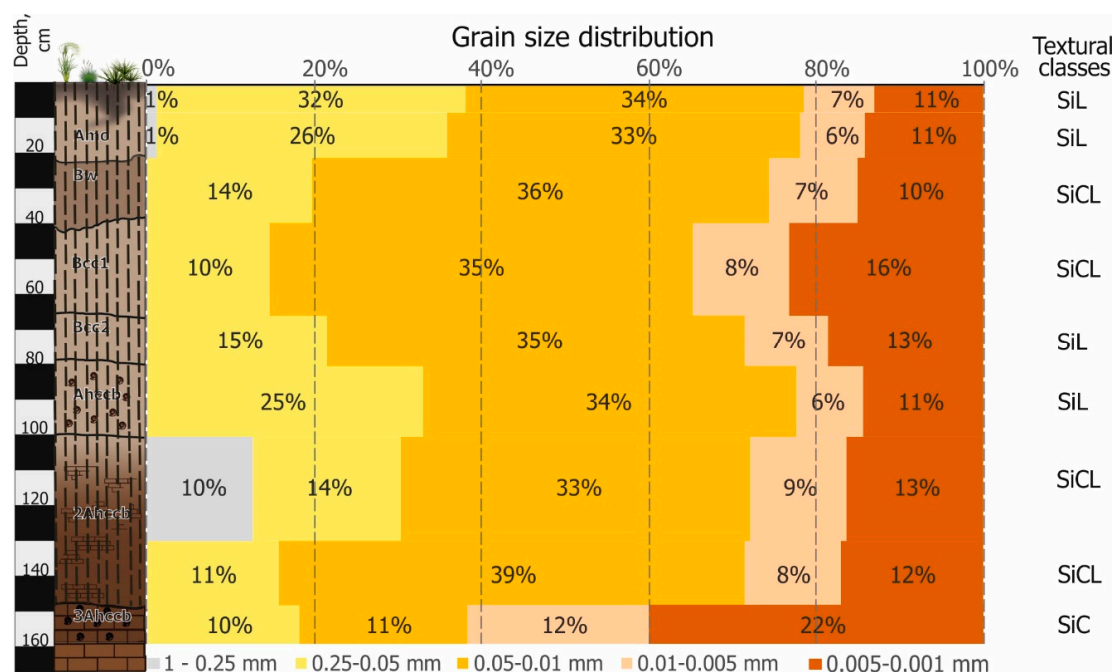


Figure 10. Grain size distribution in Calcic Kastanozem, Srednaya Akhtuba section.

Clay mineralogy. Smectites are dominant in all parts of the pedocomplex; except for the upper layer, their content decreases with depth. Illite is also abundant, comprising up to 30% of the total mineral content. Other clay minerals show slight variability (Figure 11).

Selected chemical features (Table 2). The content of organic carbon is low throughout the soil profile that is typical for Calcic Kastanozems [12]. The buried soil horizon formed in the top of the Chocolate clays shows a slight increase in TOC. The upper horizons are completely leached of carbonates; their low content is registered for the Bw horizon, while Calcic horizons show a considerable increase. Below the carbonate, contents stabilize at 6–8%. The whole pedocomplex is alkaline, with the highest values in Calcic horizons. The lower horizons are less alkaline because of chloride-magnesium-sodium salinity with gypsum. The lower loess mixed with Chocolate clays shows the highest gypsum content (3.72%) that is in line with abundant Gypsum crystals in thin sections.

The profile of Calcic Kastanozem shows a low content of soluble salts down to 100 cm. Magnesium prevails among exchangeable cations in all soil horizons except for Cambic. Chocolate clays exhibit a high content of exchangeable Sodium that results from the Sodium type of salinity.

The profile distribution of salinity is also shown in Figure 12. All soil horizons have less than 1% of non-silicate iron. A slight increase is noticed in the Cambic horizon. All layers below 100 cm show an increase in all fractions of non-silicate iron, with the maximum content in the mono-clay layer of Chocolate clays (1.72%). The fraction of crystalline iron is dominant throughout the studied pedocomplex.

Table 2. Selected chemical features of the pedocomplex.

Horizon	Depth, cm	pH _{water}	CaCO ₃ , %	TOC, g/100 g	Exchangeable Cations, % of CEC				Iron Fractions, % *				CaSO ₄ ·2H ₂ O, %	Σ of Soluble Salts, %
					Ca ²⁺	Mg ²⁺	Na ⁺	K ⁺	Feo	Fed	Fec	FeO/Fed		
Amo	0–9	8.0	0.0	1.49	45.2	51.7	1.0	2.1	0.12	0.87	0.75	0.14	n.d.	0.24
	9–20	8.2	0.0	1.20	45.6	52.1	0.8	1.5	0.09	0.98	0.89	0.09	n.d.	0.12
Bw	20–40	8.3	1.30	0.89	60.8	37.4	0.7	1.1	0.10	1.12	1.02	0.09	n.d.	0.13
		8.7	16.6	n.d.	48.7	48.7	1.1	1.5	0.11	0.80	0.69	0.14	n.d.	0.30
Bcc1	40–65	8.7	17.8	0.52	36.6	61.0	1.5	1.0	0.10	0.85	0.75	0.12	n.d.	0.20
		8.4	11.0	n.d.	38.5	57.7	2.3	1.5	0.18	0.94	0.76	0.19	n.d.	0.19
Ahccb	80–100	8.2	6.6	0.35	32.0	64.0	2.7	1.4	0.10	0.94	0.84	0.11	0.00	0.31
2Ahccb	100–148	8.0	7.8	0.28	49.1	43.6	6.0	1.3	0.23	1.20	0.97	0.19	3.72	1.79
		8.1	8.0	n.d.	34.5	57.5	6.7	1.3	0.24	1.10	0.86	0.22	2.43	1.82
3Ahccb	148–160	8.1	6.0	0.49	39.1	44.7	14.5	1.6	0.43	1.72	1.29	0.25	1.86	2.57

* Iron fractions: Fed: dithionite-extractable iron; Feo: oxalate extractable iron; FeO/Fed: iron activity index; Fec = Fed – FeO: crystalline iron content.

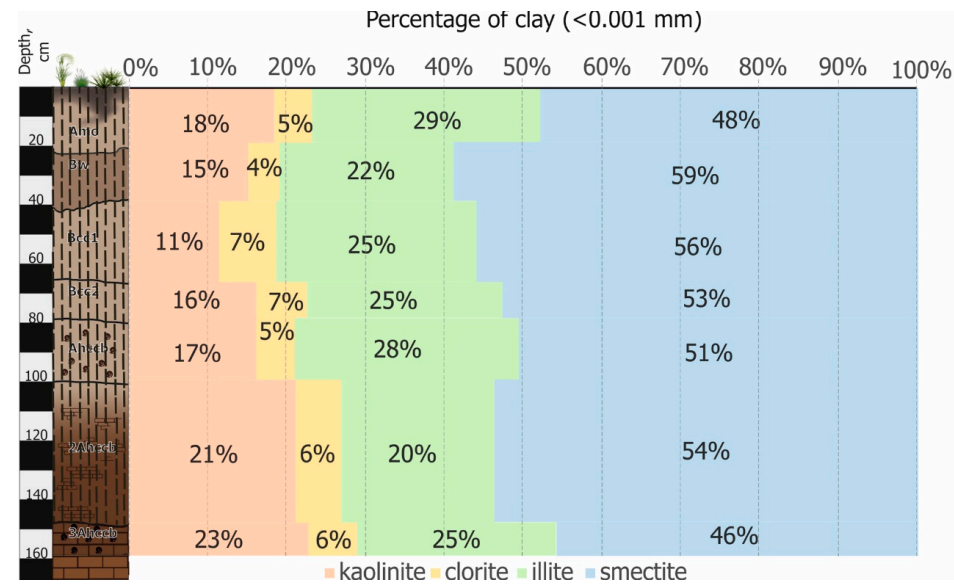


Figure 11. Clay minerals, percentage of total clay contents in Surface Kastanozem, Srednaya Akhtuba section.

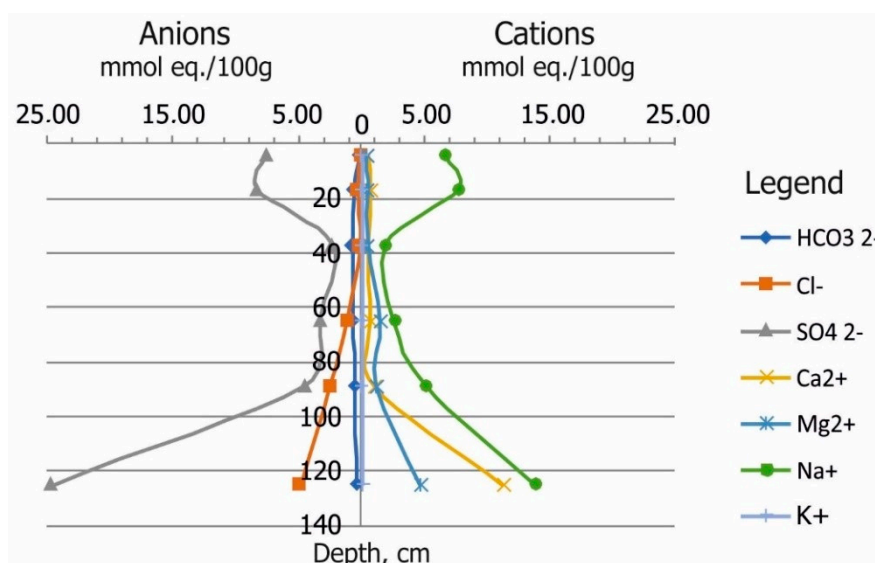


Figure 12. Distribution of salts in water extract.

5. Discussion

Sedimentology of the pedocomplex. Field morphology, micromorphology, and grain size distribution show that the studied Kastanozem is formed in a pedocomplex consisting of a layer of loess (down to 100 cm) underlain by Chocolate clays below 148 cm. Grain size differential curves clearly show the shift from marine to aeolian sedimentation by two peaks for the upper and lower part of the pedocomplex (Figure 13). The layer between 100 and 148 cm is represented by loess with an abundant admixture of clay fragments. A grain size analysis made by the pipette method (Figure 10) shows its similarity to the overlying loess. However, the differential curve is similar to the underlying clay, with a slight increase in silt (110–130, Figure 13).

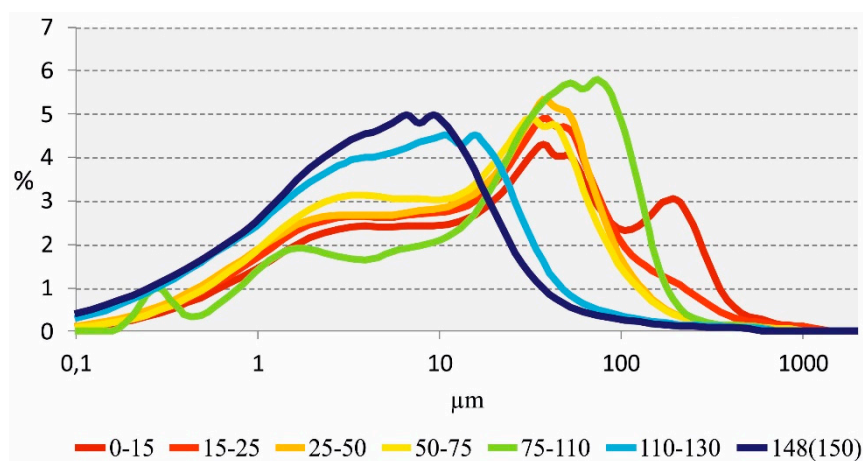


Figure 13. Grain size differential curves for various parts of the pedocomplex with Calcic Kastanozem.

Marine sedimentation. The Chocolate clays are presented by the poly-mineral formation that exhibits features typical for marine sedimentation. Brackish-water Khvalynian fauna is abundant in sandy interlayers. Mono-clay layers are Silty Clay almost without sand and a low content of Course Silt. They show high birefringence and monostriated b-fabric of the micromass inherited from clay sedimentation in the still water, like lagoon traps (Figure 6B). Micromorphology confirms that mono-clay layers also have a layered microstructure and could be subdivided into three sub-facies, including fine silty and coarse-silty micro-layers indicating variable sedimentation environments diagnostic for Chocolate clays [17,22,40]. Tudryn et al. [20] point out that these sediments suggest

a rather calm depositional environment and visually, may resemble varied sediments in periglacial lakes. They have a high content of non-silicate iron fractions that are responsible for their specific Chocolate color (Table 2)—the presence of iron oxides (hydro goethite and manganese) impregnating the entire clay series. Hydrochloric acid extracts show iron sesquioxides in clays, Fe_2O_3 in particular [41]. X-ray diffraction indicates the presence of Smectites as dominant clay minerals in Chocolate clays—they comprise about half of the clay mineral contents (Figure 11). The percentage of Illite is also high in all horizons of the pedocomplex. As was shown earlier, clay mineralogy is similar to recent terrigenous materials of the Volga River [4,7]. However, the dominant content of Illite (up to 80%) was not registered in our study. This is because we only studied the upper part of the strata of Chocolate clays formed after 12 cal kyr BP, where Illite decreases and Smectites increases and becomes the dominant mineral.

Sub-areal sedimentation. The loess layer on top of Chocolate clays exhibits properties typical for aeolian sediments—a vertical wall in the exposure, typical grain size distribution with dominant loess fractions (Coarse Silt and Fine Sand), and high porosity. The loess obviously resulted from local aeolian transportation, with the source material primarily derived from the rewinding of marine sediments. Micromorphology shows that the fragments of Chocolate clays are evenly dispersed in the micromass up to the top of the loess stratum. The fragments have the predominant size of fine sand and coarse silt (dominant loess fractions) and were mobilized by winding together with other dust grains. The high content of clay fragments is probably responsible for the heavy texture of loess. The difference in the admixture of clay fragments resulted in some variability in grain size distribution. Another piece of evidence of the local source of dust is the presence of marine component (glauconitic sand and silt grains—[42]), absent in Chocolate clays. The high content of Magnesium (water soluble and exchangeable) also points to a marine source of dust material. The high salinity of a similar type (Chloride-Magnesium-Sodium with Gypsum) evidences marine genesis for both Chocolate clays and source material for loess sediments. The local source for loess sediments is also indicated by the similar clay mineralogy in loess and Chocolate clays (Figure 11). Most of the sand grains are not rounded, showing local transport. The upper 20 cm of loess is enriched with fine sand (Table 2, Figure 13). Micromorphology shows that sand grains look similar to those in the lower horizons. Thin sand streaks could indicate either an unstable regime by the end of aeolian sedimentation or modern aeolian dusting near the cliff.

The shift from marine to sub-areal sedimentation. The composition of the pedocomplex reveals the complex history of the retreat of the sea and shift from marine to sub-areal sedimentation. As shown previously, the regressive tendency of the Late Khvalynian sea-lake was characterized by a series of minor secondary transgressive phases [23]. During the Late Khvalynian time, the northern part of the Lower Volga region was characterized by continental (subaerial) sedimentation [15]. Micromorphological studies show that there was a break between marine and subareal sedimentation stages.

Buried soil horizons are among the key evidence of break-in sedimentation. The upper layer of Chocolate clays (148–160 cm) has a complicated structural organization. Initial plates are disordered and obviously transformed by pedogenesis—a violation of initial rock fabric by a complex of biogenic, cryogenic features and gypsum crystal crystallization. The fine granular microstructure (Figure 6A,B) could have a polygenetic genesis, being the result of salt coagulation of clay and/or deep-freezing. Some of the microaggregates look like coprolites (Figure 6C,D). This is in contrast with the microfeatures of the deep layers of Chocolate clays, which had not been touched by pedogenesis (Figure 14).

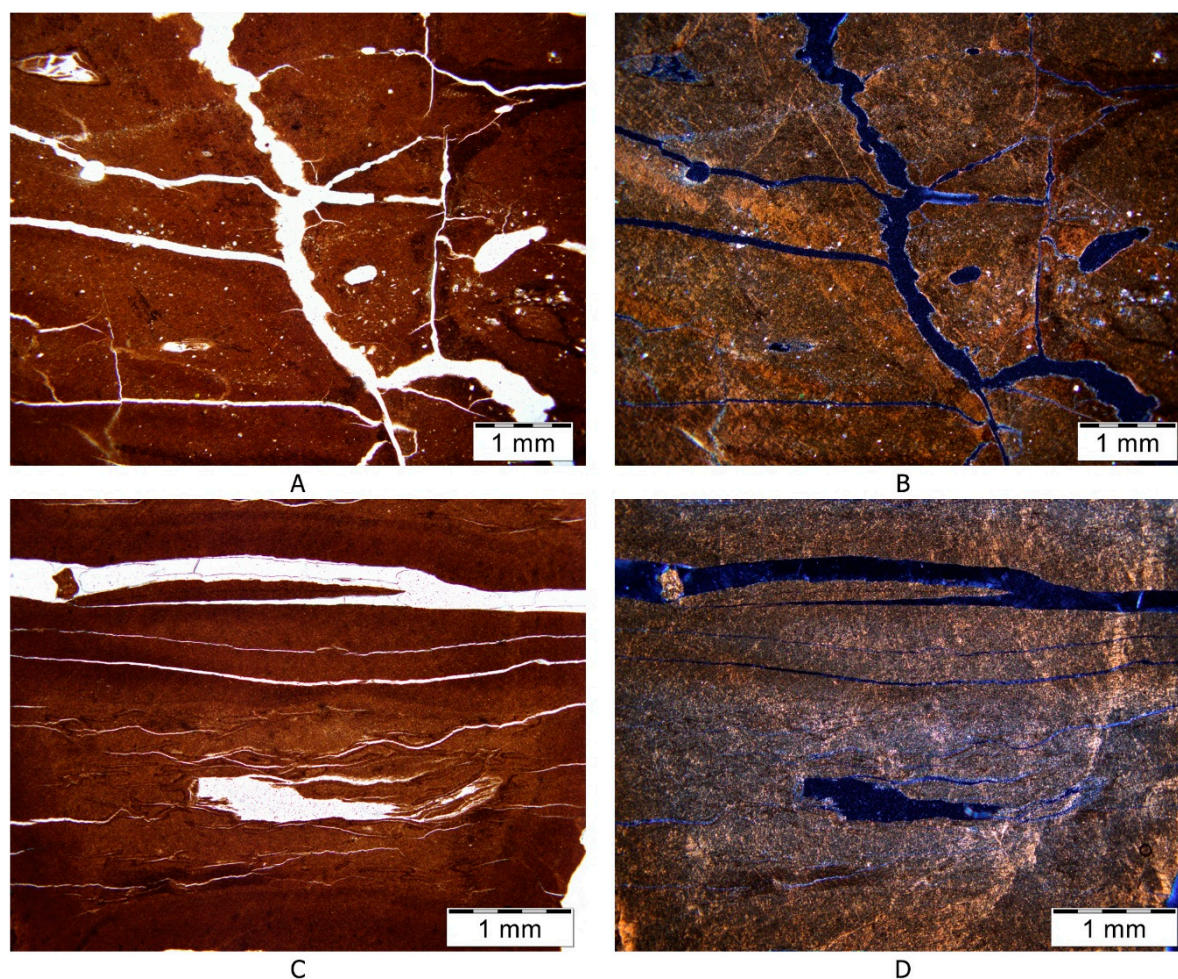


Figure 14. Microstructure of mono-clay layers of Chocolate clays untouched by pedogenesis. Left—PPL; right—XPL. (A,B)—Leninsk exposure, 25 km East of Srednaya Akhtuba section, right side bank of Akhtuba River, 231–236 cm; (C,D)—Raigorod exposure, 20.

The upper layer of Chocolate clays in the studied pedocomplex also shows the presence of a micro-zonal accumulation of small coal particles and biogenic pores, compact gypsum infillings, and thin coatings (Figure 6A,B). Big gypsum crystals with an irregular shape are relic features. Soil solutions saturated with Ca^{2+} and SO_4^{2-} needed for their crystallization could circulate exclusively with the high stand of ground water [43] that was not the case after the Early Khvalynian time. After the cease of marine sedimentation, big gypsum crystals with jagged edges were formed in the process of local re-crystallization. Infillings with diamond-shaped gypsum crystals were formed in adjacent pores (Figure 6E). Crystallization of gypsum crystals enhanced the destruction of initial clay plates on separate fragments of a smaller size. Another factor of destruction is soil biota activity (Figure 6F).

The beginning of subareal sedimentation was accompanied by mixing of the topmost disordered layer of clays with loess material and synlithogenic soil formation. The microfeatures display a fine granular microstructure. Signs of former biota activity include bio-tubulars and biogenic pores—channels (Figure 6G,H). Some of the fine grain aggregates are earthworm coprolites. The overlying layer of loess (80–100 cm) has abundant signs of ancient pedogenesis—carbonaceous fragments of plant tissue and spores (Figure 6C), bacterial iron colonies (Figure 6D), clay-humus microaggregates and clay films around silicate grains (Figure 6C,E), abundant fragments of clays assimilated in the micromass (Figure 6A), and big biogenic clay-carbonate aggregates (Figure 6F).

The *chronological framework* is based on published radiocarbon and OSL dates [19,29,31]. Based on OSL dates for the Srednaya Akhtuba section, the “marine” stage, corresponding to the Early

Khvalynian, transgression of the Caspian Sea started with the accumulation of Chocolate clays interbedded with sands at $15,000 \pm 100$ [22]. This confirms that the accumulation of Chocolate clays occurred during the degradation of Ostashkov (Late Weichselian) glaciation when the meltwater from the Scandinavian Ice Sheet margin supplied the Caspian Sea that led to the Khvalynian transgressive stage and Chocolate Clays deposition [4]. The upper layer of Chocolate clays gives the time of shift from marine to sub-areal sedimentation at $13,000 \pm 500$ years [22]. The dating material was taken from the lower part of the loess layer mixed with Chocolate clays at a depth of 145 cm that was regarded as a roof of Chocolate clays. According to Arslanov et al. [23], the transgressive stages of the Late Khvalynian basin with the sea level at about 0 m and 12 m occurred 14–12 ka cal BP. The Late Khvalynian transgression coincided with increasing aridity in the Caspian region. This is shown in the change of pollen of woody vegetation (pine, alder, birch, oak, hornbeam, willow) towards xerophilous grassy pollen typical of semi-desert and steppe vegetation [44]. During that time, the northern part of the Lower Volga region was characterized by subaerial sedimentation, during which the buried soil horizon started to form above the roof of Early Khvalynian Chocolate clays. Increasingly continental climatic conditions during the Boreal period of the Holocene resulted in the Mangyshlak regression [45,46]. Pedogenesis that started during the time of the shift from marine to subareal sedimentation then accompanied sedimentation of the lower part of loess sediment. This led to the development of the buried soil in the roof of Chocolate clays and two synlithogenic soils at 100–148 and 80–100 cm. The properties of these buried soils support paleogeographic reconstruction for the time of the last deglaciation made on the basis of pollen analyses as an arid and cold environment.

The OSL dating of the lower part of the loess layer in the Srednaya Akhtuba section gives an age of 9.6 ± 0.6 ka [16]. Although this quartz age appears to be sufficiently reset (given the IR50 age of 9.0 ± 0.5 ka), the age may not be accurate. This dating material is a mixture of the bioturbated upper layer of Chocolate clays and loess. The loess component was most likely to have been daylight exposed before deposition [47–49]. The clay component was probably not further exposed to light after primary marine deposition, but reworked in such a manner as to retain more or less all of its quartz OSL and feldspar IRSL signals. However, this material was mixed with well-reset loess, to give an age younger than that of the underlying Chocolate clays. The OSL date for the lower part of the Mollic horizon is 720 ± 70 ka [16], which could be explained by the modern rewinding of loess material, also confirmed by grain size distribution (Figures 10 and 11).

Modern pedogenesis. The surface Calcic Kastanozem is a full Holocene soil developed in subareal post-Khvalynian sediments starting from the Boreal time. It has a set of features typical for Kastanozems and reflects the present environmental conditions. The light colored Mollic horizon is leached from carbonates. Due to a continental climate, the soil experiences winter freezing with a lack of snow and sparse vegetation. For this reason, the Mollic horizon is subjected to a modern cryogenic impact (crashed sand grains with their circular orientation, Figure 8D). The upper part of the Mollic horizon has uncoated coarse grains due to leaching. The Cambic horizon is leached from soluble salts and has a low content of carbonates. It is well-structured, with high birefringence in the micromass and with thin fragmented clay coatings. These features are also in line with a modern continental climate. In spring after the snowmelt and in autumn with abundant rainfall, the soil receives enough moisture to provoke the leaching of carbonates, resulting in high mobility of the soil matrix. Calcic horizons are also well-structured, with abundant earthworm casts (Figure 7A,B). A high carbonate content is presented by strong micritic impregnation of the micromass and abundant hard nodules with diffuse boundaries. There are signs of progressive aridization within the upper 40 cm: a–upward movement of carbonates from lower horizons is indicated locally by loose infillings in inner-pedal voids (Figure 8A,B) and plant residues (Figure 8G,H); b–upward accumulation of soluble salts (sodium sulfates, Figure 11). The lower horizons of Kastanozem are presented by buried horizons of Boreal and Late Pleistocene (MIS2) paleosols.

6. Conclusions

1. The complex study of surface Calcic Kastanozem in the exposure of Srednaya Akhtuba shows that it developed in a pedocomplex that formed between the time of the last deglaciation and Boreal time. The pedocomplex includes a layer of loess underlain by Chocolate clay. The loess exhibits properties typical for aeolian sediments and indicates the local source for aeolian transport (enrichments in fragments of Chocolate clays and glauconitic grains, the similarity in clay mineralogy and the type of salinity). Chocolate clays influence the composition of the upper loess layer, e.g., clay fragments are responsible for its heavy texture and high gypsum content.
2. The shift from marine to subareal sedimentation was a complex process accompanied by breaks that made the development of buried horizons of synlithogenic soils possible.
3. The features of shallow buried soil horizons confirm increasing aridity during the Late Khvalynian, and after the Khvalynian time up to the Boreal period. The lower part of surface Calcic Kastanozem (below 100 cm) is superimposed on shallow buried soil horizons of cryoarid soil.
4. Surface Calcic Kastanozem fully reflects modern climatic conditions of the dry steppe. However, it is deeply influenced by shallow buried soils and Chocolate clays.
5. Srednaya Akhtuba is a unique exposure, with both marine and continental sediments of the time of the last deglaciation. The results of this study could be further used for broader paleoclimatic reconstructions for the whole Ponto-Caspian area.

Author Contributions: For research articles with several authors, a short paragraph specifying their individual contributions must be provided. The following statements should be used “conceptualization, A.M., M.L., T.Y., and A.R.; methodology, P.K., T.R., A.R., and R.K.; validation, R.K., T.Y., M.L., and E.V.; formal analysis, E.V., P.K., and T.R.; investigation, T.R., R.K., A.R., A.M., M.L., and P.K.; data curation, T.R.; writing—original draft preparation, A.M., M.L., and T.R.; writing—review and editing, A.M., M.L., and T.R.; visualization, T.R.; supervision, A.M. and M.L.; project administration, M.L.”.

Funding: This research was supported by the Russian Foundation for Basic Research (Project No. 18-04-00638). Laboratory studies were performed with equipment of the Center for Collective Use of Scientific Equipment “Functions and Properties of Soils and Soil Cover” of the V.V. Dokuchaev Soil Institute.

Conflicts of Interest: The authors declare no conflict of interest.

References

1. Yanina, T.A. The Ponto-Caspian region: Environmental consequences of climate change during the Late Pleistocene. *Quat. Int.* **2014**, *345*, 88–99. [[CrossRef](#)]
2. Svitoch, A.A. Khvalynian transgression of the Caspian Sea was not a result of water overflow from the Siberian Proglacial lakes, nor a prototype of the Noachian flood. *Quat. Int.* **2009**, *197*, 115–125. [[CrossRef](#)]
3. Svitoch, A.A. The Neoeuxinian basin of the Black Sea and the Khvalinian transgression of the Caspian Sea. *Quat. Int.* **2010**, *225*, 230–234. [[CrossRef](#)]
4. Tudryn, A.; Leroy, S.A.; Toucanne, S.; Gibert-Brunet, E.; Tucholka, P.; Lavrushin, Y.A.; Dufaure, O.; Miska, S.; Bayon, G. The Ponto-Caspian basin as a final trap for southeastern Scandinavian Ice-Sheet meltwater. *Quat. Sci. Rev.* **2016**, *148*, 29–43. [[CrossRef](#)]
5. Zhukov, M.M. The differential vertical movements of the shores of the Caspian sea in Quaternary time. *Uch. Zap. Mosc. State Univ. Geogr.* **1941**, *48*, 25–32. (In Russian)
6. Britsyna, I.P. *Distribution of the Khvalynian Chocolate Clays and Problems of the Paleogeography of the North Caspian Region*; Institute of Geography, Academy of Sciences of the USSR: Moscow, Russia, 1954; Volume 62, pp. 5–27. (In Russian)
7. Makshaev, R.R.; Svitoch, A.A. Chocolate clays of the Northern Caspian Sea Region: Distribution, structure, and origin. *Quat. Int.* **2016**, *409*, 44–49. [[CrossRef](#)]
8. Bolshakov, A.F.; Borovsky, V.M. Soils and microrelief of the Caspian lowland (according to the materials of the Dzhanybek stationary of the Soil Institute of the Academy of Sciences of the USSR). In *Materials of Surveys, Studies and Design of the Volga Irrigation: “Solontsy of the Volga Region”*; Publishing House of the Academy of Agricultural Sciences: Moscow, Russia, 1937; Volume 7, pp. 134–169. (In Russian)

9. Budina, L.P. Meadow brown semidesert soils. In *Genesis and Classification of Semidesert Soils*; Nauka (USSR): Moscow, Russia, 1966; pp. 59–72. (In Russian)
10. Ivanova, E.N. (Ed.) *Soils of the Complex Northern Caspian Plain and Their Characteristics for Reclamation Purposes*; Nauka: Moscow, Russia, 1964.
11. Kovda, V.A. *Soils of the Caspian Lowland*; Izd. Akad. Nauk SSSR: Moscow, Russia, 1950; p. 249. (In Russian)
12. Rode, A.A.; Pol'skij, M.N. Soils of the semi-desert of the North-Western Caspian region and their reclamation. In *Proceedings of V.V. Dokuchaev Soil Science Institute*; USSR AS Publishing: Moscow, Russia, 1961; Volume 56, pp. 3–214. (In Russian)
13. Sotneva, N.I. The dynamics of climatic conditions at the Dzhanybek Research Station in the northern Caspian Lowland in the second half of the XXth century. In *Izvestiya RAN; Geographical Series*; Nauka: Moscow, Russia, 2004; Volume 5, pp. 74–83. (In Russian)
14. Arslanov, K.A.; Druzhinina, O.A.; Kublitsky, Y.A.; Subetto, D.A.; Syrykh, L.S. New data on Palaeoenvironment of South-Eastern Baltic region: Results of researches of 2011–2013. In *VIII All-Russian Conference on Quaternary Research: «Fundamental Problems of Quaternary, results and Main Trends of Future Studies»*; SSC RAS Publishers: Rostov-on-Don, Russia, 2013; pp. 34–36. (In Russian)
15. Thompson, W.; Kurbanov, R.; Murray, A.; Yanina, T.; Svistunov, M.; Yarovaya, S. First optically-stimulated luminescence ages of the early Khvalynian “Chocolate clays” of the lower Volga. In *Proceedings of the International Conference Loessfest 2018 Diversity of Loess: Properties, Stratigraphy, Origin and Regional Features*, Volgograd, Russia, 24–29 September 2018; pp. 122–123.
16. Kurbanov, R.N.; Murray, A.S.; Yanina, T.A.; Svistunov, M.I.; Taratunina, N.A.; Thompson, W.K. First optically stimulated luminescence ages of the Early Khvalynian Caspian Sea transgression in the Lower Volga. *Quaternary Geochronology* **2019**, *52*. in press.
17. Moskvitin, A.I. *Pleistocene of the Lower Volga Region*; Academy of Sciences of the USSR: Moscow, USSR, 1961; p. 264. (In Russian)
18. Svitoch, A.A.; Yanina, T.A. *Quaternary Sediments of the Coasts of the Caspian Sea*; RASHN: Moscow, Russia, 1997; p. 267.
19. Lavrushin, Y.A.; Spiridonov, E.A.; Tudrin, A.; Shali, F.; Antipov, M.P.; Kuralenko, N.P.; Kurina, E.E.; Tuholka, P. Caspian: Late Quarter hydrological events. *Bull. Comm. Stud. Q. Period* **2014**, *3*, 19–50.
20. Tudryn, A.; Chaliev, F.; Lavrushin, Y.A.; Antipov, M.P.; Spiridonova, E.A.; Lavrushin, V.; Tucholka, P.; Leroy, S.A.G. Late Quaternary Caspian Sea environment: Late Khazarian and Early Khvalynian transgressions from the lower reaches of the Volga River. *Quat. Int.* **2013**, *292*, 193–204. [[CrossRef](#)]
21. Makeev, A.; Rusakov, A.; Bagrova, S.; Kurbanov, R.; Yanina, T. Pedogenetic response to climatic fluctuations within the last glacial-interglacial cycle in the lower Volga basin. In *Proceedings of the IGCP 610 Fourth Plenary Conference and Field Trip from the Caspian to Mediterranean: Environmental Change and Human Response during the Quaternary*, Tbilisi, Georgia, 2–9 October 2016; pp. 111–114.
22. Yanina, T.A.; Svitoch, A.A.; Kurbanov, R.N.; Murray, A.S.; Tkach, N.T.; Sychev, N.Y. Paleogeographic analysis of the results of optically stimulated luminescence dating of pleistocene deposits of the Lower Volga area. *Vestnik Mosk. Univ. Seriya Geogr.* **2017**, *2017*, 20–28. (In Russian)
23. Arslanov, K.A.; Yanina, T.A.; Chepalyga, A.L.; Svitoch, A.A.; Makshaev, R.R.; Maksimov, F.E.; Chernov, S.B.; Tertychniy, N.I.; Starikova, A.A. On the age of the Khvalynian deposits of the Caspian Sea coasts according to ¹⁴C and ²³⁰Th/²³⁴U methods. *Quat. Int.* **2016**, *409*, 81–87. [[CrossRef](#)]
24. *Guidelines for Soil Description*, 4th ed.; Food and Agriculture Organization of the United Nations: Rome, Italy, 2006; p. 110.
25. Munsell, A.H. *Munsell Soil Color Charts: With Genuine Munsell* Color Chips*; Munsell Color Company: Grand Rapids, MI, USA, 2013.
26. IUSS Working Group WRB. *World Reference Base for Soil Resources 2014, Update 2015 International Soil Classification System for Naming Soils and Creating Legends for Soil Maps*; World Soil Resources Reports No. 106; FAO: Rome, Italy, 2015.
27. Stoops, G. *Guidelines for Analysis and Description of Soil and Regolith Thin Sections*; Vepraskas, M.J., Ed.; Soil Science Society of America Inc.: Madison, WI, USA, .
28. Kachinskiy, N.A. *Soil Physics—Part 1*; Higher Education Publishing House (USSR): Moscow, USSR, 1965; p. 321. (In Russian)

29. Kozlovskiy, F.I. Methods of Salt Regime Assessment in Soils. In *Methods of Stationary Studies of Soils*; Science Publishing House (USSR): Moscow, USSR, 1977; pp. 88–166. (In Russian)
30. Khitrov, N.B.; Ponizovskij, A.A. *Guide to Laboratory Methods for Studying the Ion-Salt Composition of Neutral and Alkaline Mineral Soils*; Vashnil, V.V., Ed.; Dokuchaev Soil Science Institute: Moscow, Russia, 1990; p. 235. (In Russian)
31. Pankova, E.I.; Vorobyova, L.A.; Gadzhiyev, I.M.; Gorokhova, I.N.; Elizarova, T.N.; Korolyuk, T.V.; Lopatovskaya, O.G.; Novikova, A.F.; Reshetov, G.G.; Skripnikova, M.I.; et al. *Salt-Affected Soils of Russia*; Akademkniga: Moscow, Russia, 2006; p. 854. (In Russian)
32. Gorbunov, N.I. *Fine Minerals and Methods of Their Investigation*; AS Publishing: Moscow, USSR, 1963; p. 302. (In Russian)
33. Mehra, O.P.; Jackson, M.L. Iron oxide removal from soils and clays by a dithionite-citrate system buffered with sodium bicarbonate. In *Clays and Clay Minerals*; Ingerson, E., Ed.; Pergamon: Bergama, Turkey, 2013; pp. 317–327.
34. Biscaye, P.E. *Mineralogy and Sedimentation of the Deep-Sea Sediment Fine Fraction in the Atlantic Ocean and Adjacent Seas and Oceans*; Department of Geology, Yale University: New Haven, CT, USA, 1964.
35. Biscaye, R.E. Mineralogy and sedimentation of recent deep-sea clay in the Atlantic Ocean and adjacent Seas and Oceans. *Bull. Geol. Soc. Am.* **1965**, *76*, 803–832. [[CrossRef](#)]
36. *X-ray Methods of Studying and the Structure of Clay Minerals*; Braun, G. (Ed.) Mir Publishing: Moscow, Russia, 1965; p. 599. (In Russian)
37. Gradusov, B.P. X-ray diffractometry method in mineralogical studies of soils. *Pochvovedenie* **1967**, *10*, 127–137. (In Russian)
38. Gradusov, B.P. *Minerals with a Mixed Structure in Soils*; USSR AS Publishing: Moscow, Russia, 1976. (In Russian)
39. Sokolova, T.A.; Dronova, T.J.; Tolpeshta, I.I. *Clay Minerals in Soils: Text Book*; Akademkniga Pub: Moscow, Russia, 2005; p. 336. (In Russian)
40. Svitoch, A.A.; Makshaev, R.R.; Rostovtseva, Y.V.; Klyuvitkina, T.S.; Berezner, O.S.; Tregub, T.F.; Khomchenko, D.S. *Chocolate Clays of the Northern Caspian Sea Region*; Faculty of Geography, Lomonosov Moscow State University: Moscow, Russia; OOO Krasnogorskaya Tipografiya: Moscow, Russia, 2017; p. 140. (In Russian)
41. Priklonsky, V.; Gorkova, I.; Oknina, N. Engineeringgeological properties of Khvalynian clays in the context of environments of their deposition. In *Trudy Laboratorii Hidrogeologicheskikh Problem*; Laboratory for Hydrogeological Problems: Moscow, USSR, 1956; Volume 13, pp. 1–152.
42. Kostov, I. *Mineralogy*; Mir: Moscow, USSR, 1971; Volume 40. (In Russian)
43. Poch, R.M.; Artieda, O.; Lebedeva, M. Chapter 10—Gypsic Features. In *Interpretation of Micromorphological Features of Soils and Regoliths*, 2nd ed.; Stoops, G., Marcelino, V., Mees, F., Eds.; Elsevier: Amsterdam, The Netherlands, 2018; pp. 259–287.
44. Abramova, T.A. Reconstruction of the Paleogeographical Environment of the Quaternary-Transgressions and Regressions of the Caspian Sea (on the Data of Paleobotany Investigations). Ph.D. Thesis, Moscow State University, Moscow, USSR, 1974. (In Russian)
45. Rychagov, G.I. *Pleistocene History of the Caspian Sea*; Moscow State University Pub: Moscow, Russia, 1997; p. 267. (In Russian)
46. Bolikhovskaya, N.S. Evolution of the Climate and Landscapes of the Lower Volga Region during Holocene. *Vestnik Mosc. Univ. Geogr.* **2011**, *2*, 13–27. (In Russian)
47. Wintle, A.G. A review of current research on TL dating of loess. *Quat. Sci. Rev.* **1990**, *9*, 385–397. [[CrossRef](#)]
48. Olley, J.; Caitcheon, G.; Murray, A. The distribution of apparent dose as determined by optically stimulated luminescence in small aliquots of fluvial quartz: Implications for dating young sediments. *Quat. Sci. Rev.* **1998**, *17*, 1033–1040. [[CrossRef](#)]
49. Hilgers, A.; Murray, A.; Schlaak, N.; Radtke, U. Comparison of quartz OSL protocols using Lateglacial and Holocene dune sands from Brandenburg, Germany. *Quat. Sci. Rev.* **2001**, *20*, 731–736. [[CrossRef](#)]

